

Revitalizing Crustacean Waste: Novel Antibacterial Carbon Dots and Copper-Doped Zinc Oxide Composite for Effective Waste Management

Lima Sebastian¹ and Ushamani Mythili²

Department of Chemistry and Centre for Research^{1,2}

St. Teresa's College (Autonomous), Ernakulam, Kerala, India

Corresponding Author-ushamanim@teresas.ac.in (ORCID-0000-0002-2861-4886)²

Abstract: *This research article presents a comprehensive investigation into the synthesis, characterization, and antibacterial activity of novel nanocomposite of Carbon dot with Copper doped Zinc Oxide. Fluorescent carbon dots were successfully synthesized from prawns shell waste via hydrothermal method and characterized through XRD, TEM, UV-Visible spectroscopy, and FTIR analysis, confirming their size, morphology, and functional groups. Concurrently, zinc oxide and copper-doped zinc oxide nanoparticles were synthesized and characterized, demonstrating changes in crystal size, morphology, and elemental composition upon copper doping. It was further made into nanocomposite with carbon dot. The primary focus of this study was on the antibacterial properties of these materials. A comparative analysis revealed that the carbon dot@ZnO-Cu nanocomposite exhibited significantly enhanced antibacterial activity against *E. coli* and *S. aureus* when compared to carbon dots alone and carbon dot@ZnO nanocomposite. These findings underscore the potential of this novel nanocomposite for advanced antibacterial applications.*

Keywords: Carbon dot, Nanocomposite, Crustacean waste, Antibacterial activity.

I. INTRODUCTION

The growing threat of bacterial and fungal infections has created an urgent need for innovative antibacterial materials to address the escalating global health challenges. The emergence of multiple drug-resistant (MDR) bacteria due to prolonged antibiotic use and the devastating impact of pathogens on health necessitate effective solutions that mitigate these risks while minimizing environmental harm. In this context, carbon-based nanomaterials have surfaced as a promising avenue, driven by their benign nature, abundance, and cost-effectiveness. Among these, carbon dots (CDs), with diameters below 10 nm, have demonstrated remarkable potential as antibacterial agents.[1-3]

Carbon dots, renowned for their size-dependent high fluorescence properties, emerged serendipitously during the purification of single-walled carbon nanotubes in 2004. They exhibit a wide range of characteristics that have aroused a great deal of curiosity in several scientific domains. Their fascinating antibacterial action and underlying processes, in particular, have attracted interest in the fields of medical and environmental applications. Recent research has revealed that carbon dots naturally possess the capacity to successfully stop bacterial development. The rupture of bacterial cell membranes, the creation of oxidative stress, and interference with crucial enzyme processes are few of the proposed mechanisms that contribute to this antibacterial activity. Carbon dots and bacteria interact to cause membrane permeabilization, which compromises cellular integrity and causes bacterial mortality. Additionally, reactive oxygen species photogenerated by carbon dots add to oxidative damage, hastening the death of bacteria. This study focuses on exploiting waste from marine crustaceans, particularly prawns shells, to create fluorescent carbon dots through hydrothermal process that is environmentally benign.[2, 4-10]

Marine crustacean waste, generated from industries like seafood processing and aquaculture, presents a significant environmental challenge in terms of disposal. The disposal of such waste can lead to detrimental effects on marine ecosystems and coastal environments. Improper disposal methods, such as dumping waste into oceans or coastal waters,

can result in various ill effects. The economic implications of improperly managed waste are significant as well, as polluted waters can damage fisheries, tourism, and coastal economies.[11-13] Converting shellfish waste, particularly chitin-rich prawn shells, into fluorescent carbon dots through an affordable hydrothermal process offers an inventive approach to recycling waste and creating valuable materials.

Zinc oxide (ZnO) has gained significant attention due to its impressive ability to combat bacteria effectively and its compatibility with living organisms. The integration of zinc oxide (ZnO) nanoparticles with carbon dots in a composite structure holds the potential for significantly enhanced antibacterial activity. This combines the inherent properties of both materials to create a synergistic effect that can combat bacterial infections more effectively. Zinc oxide nanoparticles are known for their intrinsic antibacterial properties, attributed to their ability to generate reactive oxygen species (ROS) when exposed to light or in the presence of moisture. These ROS cause oxidative stress and damage to bacterial cell membranes and DNA, leading to bacterial cell death. Additionally, zinc ions released from the ZnO nanoparticles can further hinder bacterial growth. Carbon dots, on the other hand, possess unique surface chemistry and can be easily functionalized. When integrated with ZnO nanoparticles, they can enhance the composite's stability, biocompatibility, and interaction with bacterial cells. Carbon dots can also contribute to the generation of additional ROS under specific conditions, augmenting the oxidative stress on bacteria.[14-17]

The antibacterial effects of CD@ZnO nanocomposites have not received sufficient investigation. Particularly, the exploration of CDs combined with copper-doped ZnO nanocomposites (CD@ZnO-Cu) remains largely unexplored in existing research. Addressing this gap, the present study aims to provide insights into this area. We have successfully synthesized CD@ZnO nanocomposites as well as CD@ZnO-Cu nanocomposites, and we conducted a thorough assessment of their antibacterial capabilities, specifically in the presence of visible light conditions. This study presents novel antibacterial materials derived from crustacean waste, presenting sustainable options for both healthcare and environmental conservation.

II. MATERIALS AND METHODS

2.1 Materials

Sodium hydroxide (NaOH), Hydrogen chloride (HCl), Glacial acetic acid, Zinc Acetate ($\text{Zn}(\text{CH}_3\text{COO})_2 \cdot 2\text{H}_2\text{O}$), Copper Nitrate ($\text{Cu}(\text{NO}_3)_2 \cdot 3\text{H}_2\text{O}$), Potassium Hydroxide (KOH) were purchased from Alpha Chemicals Pvt. Ltd, Kochi, Kerala. The prawn shell waste was collected from house hold kitchen wastes. All chemicals were of analytical grade. Distilled water was used throughout for all experiments.

2.2 Methods

2.2.1 Synthesis of Carbon dot

The prawn shell was washed with water and dried in day light for one week. The dried shells were ground by using mixer grinder to make the fine powder. The powdered prawn shells were again washed with distilled water. The cleaned samples were dried overnight at 80 °C. 2.0 g of dried prawn shell powder was treated with 25 mL of 3% NaOH solution at room temperature for 5 h. The powder washed with deionized water followed by centrifugation until a neutral pH was obtained. The sample was treated with 1% hydrochloric acid solution for 6 h at room temperature. After acid treatment, the sample was washed with deionized water and centrifuged several times to obtain a neutral pH. The prawn shells were transferred to a 50% sodium hydroxide solution and refluxed at 80 °C for 2 h. The refluxed sample was cooled down to the room temperature and filtered through Whatman filter paper. The obtained product was dispersed in 25 mL of 2% acetic acid solution. Then the sample was transferred to stainless steel autoclave and kept at 200 °C for 8 h. The C-dots were collected, centrifugation for one hour followed by suction filtration using polyvinylidene difluoride (PVDF) membrane. The sample were used for further characterization purpose.[13]

2.2.2 Synthesis of ZnO Nanoparticles

Zinc oxide nanoparticles were synthesized through precipitation method. To the aqueous solutions of zinc acetate (0.1 M) sodium hydroxide solution (0.1 M) was added slowly in drops (0.5 ml/min), under vigorous stirring. The reaction was kept overnight for stabilization. It was then centrifuged at 6000 rpm for 25 minutes and washed with distilled

water. The nanoparticles were dried in an oven at 60°C for 14 h. After drying nanoparticles, were ignited in a muffle furnace at 500°C for 15–20 min. The ignited nanoparticles were stored under airtight conditions.[18]

2.2.3 Synthesis of Cu doped ZnO Nanoparticles

Cu-doped ZnO nanoparticles were synthesized using the co-precipitation process. 200 ml of an aqueous mixture of zinc and copper precursors was used at Cu : Zn molar ratio of 1:9 for 10% Cu doped ZnO. The aqueous NaOH was slowly dropped into the mixture solution while stirring with a magnetic stirrer until the pH value reached 14. Precipitate formed in the solution was kept overnight. After that, the precipitate was washed with distilled water and centrifuged at 6000 rpm for 20 minutes. Then the precipitate was oven dried at 120⁰ C for 12 hours.[19]

2.2.4 Synthesis of C-dot@ZnO Nanocomposite

0.1g of synthesized ZnO was dissolved in 20 ml solution of previously prepared CDs and stirred for 15 min at room temperature, then transferred into the autoclave to react for 3 hr at 100⁰C. The obtained nanocomposite were used for further studies.[20]

2.2.5 Synthesis of C-dot@ZnO-Cu Nanocomposite

0.1g of synthesized Cu-doped ZnO nanoparticle was dissolved in 20 ml solution of previously prepared CDs and stirred for 15 min at room temperature, then transferred into the autoclave to react for 3 hr at 100⁰C. The obtained composite were used for further studies.

2.2.6 Antibacterial Activity Assay

The antibacterial activities of the C-dot, C-dot@ZnO and C-dot@ZnO-Cu were assessed by agar well diffusion method. One ml of the fresh culture of *E.Coli* and *Staphylococcus* was inoculated in the sterile Petri dishes distinctly. Wells were made using a sterile cork borer into agar plates containing inoculums. Then, 100 µl of each test solution was added to respective wells. The test solutions were C-dot(D), Cdot@ZnO(E) and C-dot@ZnO-Cu(F). Then, the plates were incubated at 37°C for 24 hours. Antimicrobial activity was detected by measuring the zone of inhibition (including the diameter of the wells) that appeared after the incubation period. Acetic acid was employed as a negative control. Tetracycline, an antibiotic was used as a standard.

III. RESULTS AND DISCUSSIONS

3.1 Characterisations of Carbon Dots

3.1.1 UV-visible Spectroscopy

Examination of the fluorescent C-dots was conducted through UV-Vis spectroscopy, providing valuable insights into their optical properties. The UV-Vis spectra unveiled the presence of two absorption peaks (Figure1).Notably, a well-defined and sharp absorption peak was observed at 280 nm.

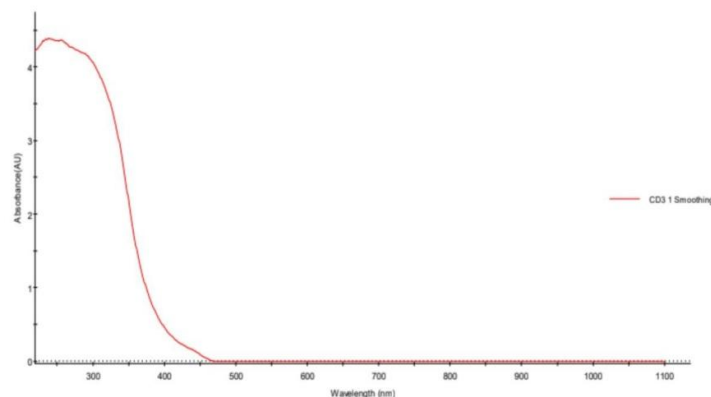


Fig 1: UV spectrum of carbon dot

Another absorption feature appeared around 330 nm, exhibiting a relatively flatter profile. These peaks were attributed to the intricate electronic transitions occurring at the surface of the C-dots. The absorption peak at 280 nm can be attributed to $\pi \rightarrow \pi^*$ electronic transitions. On the other hand, the absorption around 330 nm corresponds to $n \rightarrow \pi^*$ electronic transitions. [21, 22]

3.1.2 Fluorescence Study

Upon preparation, the C-dot solution exhibited a yellowish hue when exposed to normal light conditions. However, its behavior took on a captivating transformation when subjected to UV excitation. Within a UV-illuminated environment, the solution radiated a green fluorescence as shown in Figure 2, illustrating its unique optical properties. [23]



Fig2: Fluorescence of carbon dot observed in UV Chamber

3.1.3 FTIR studies

Fourier Transform Infrared (FTIR) spectroscopy was employed to delve into the surface groups and structural characteristics of the synthesized carbon dots (C-dots) derived from prawn shells. This technique enabled the exploration of chemical bonding within the sample by examining its absorption of infrared radiation. Notably in figure 3, an absorption band within the range of $3400\text{--}3100\text{ cm}^{-1}$ is seen, showing the presence of either --OH or --NH stretching of surface functionalities. Concurrently, a weak band is seen in the $2200\text{--}2000\text{ cm}^{-1}$ range, suggestive of the presence of a nitrile group. The FTIR analysis further unveiled a significant absorption band spanning $1550\text{--}1650\text{ cm}^{-1}$, indicative of --NH_2 groups via amide (--C=O) bonds. It's noteworthy that this absorption region also encompassed contributions from other functional groups, including C=C vibrations characteristic of aromatic compounds, non-aromatic double bonds, and the hydrogen bonds of the C=O groups found in ketones, Symmetric stretching of the COO- group. Another observation was the absorption peak at 1412 cm^{-1} , which aligned with the symmetrical deformations of the CH_3 group. Meanwhile, a distinctive narrow band emerged at 1018 cm^{-1} , revealing the presence of --C--O--C linkages. [24, 25]

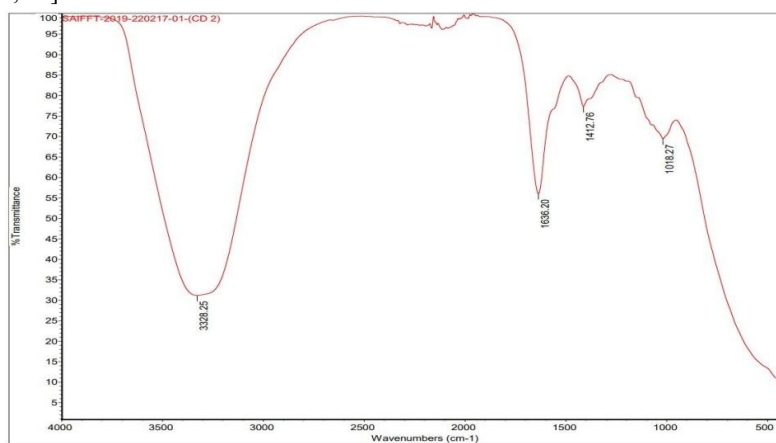


Fig 3 : FTIR spectrum of C-dot

3.1.4 TEM

Transmission Electron Microscopes (TEM) was done to unravel the morphological attributes and dimensions of the synthesized Carbon dots. The TEM images of the carbon dots showcased their uniformity, showing its homogenous nature. Evidently, the particles assumed a spherical configuration, as evidenced in Fig 4(a) The diameter range of these CDs spanning from 8 to 9 nm, as depicted in Fig 4(b). [26]

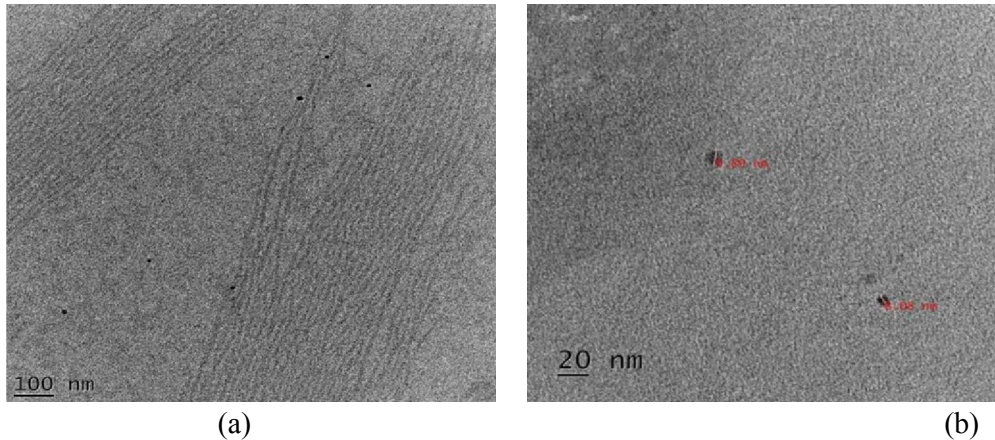


Fig 4: TEM image of carbon dot

3.2 Characterizations of ZnO Nanoparticles

3.2.1 X-ray diffraction

The crystal sizes of ZnO nanoparticles was analyzed using XRD studies. Figure 5 shows the XRD spectrum of synthesized ZnO nanoparticles. To quantify the average crystal size, the Debye Scherrer equation was employed

$$D = 0.9 \lambda / B \cos \theta$$

Where B is the full width at half maximum (FWHM) and θ is the angle of the maximum peak and λ is the wavelength of the source. The average crystal size was found to be 13.252 nm. This confirms that the particles belongs to nanoparticle range. XRD peaks at 2θ values of 31.863, 34.476, 36.333, 47.594, 56.689, 62.843, 66.393, 67.954, 69.117, and 77.028, these can be correlated with the respective crystal planes of (100), (002), (101), (102), (110), (103), (200), (112), (201), and (202). These findings intricately outline the hexagonal crystal geometry inherent to the ZnO nanoparticles' structure, shedding light on their crystalline arrangement. [27, 28]

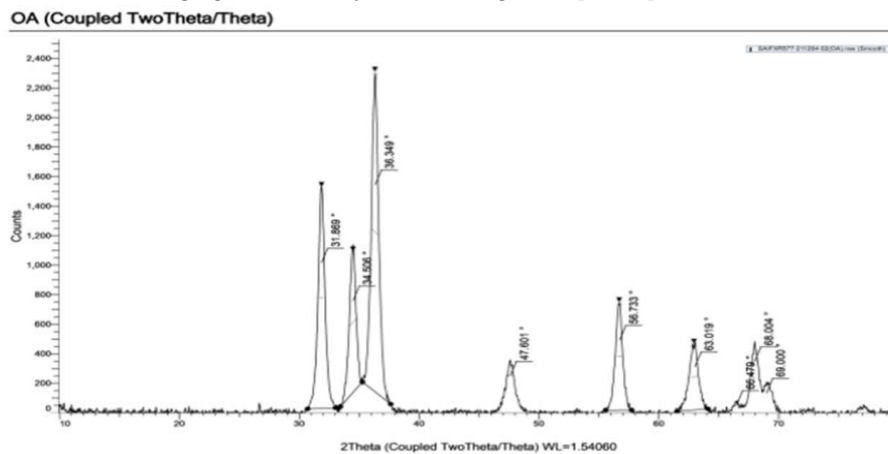


Fig. 5: XRD spectrum of Zinc Oxide nanoparticles

3.2.2 FTIR studies

Fourier Transform Infrared (FTIR) analysis was conducted to unravel the functional groups present within the synthesized ZnO nanoparticles. The spectrum prominently exhibits key absorption features that encapsulate the distinctive chemical associations within the ZnO nanoparticles. The absorption peak observed at 425.32 cm^{-1} , corresponds to the characteristic Zn-O bond (ZnO stretching vibration). This peak serves as a fingerprint of the structural arrangement between zinc and oxygen atoms, shedding light on their interconnectedness. A broad peak at 3426 cm^{-1} , it is indicative of the characteristic absorption of hydroxyl groups. The absorption peaks located at 1384.43 cm^{-1} and 1628.72 cm^{-1} symmetric and asymmetric O-C-O stretching vibration of adsorbed carbonate anion respectively(Figure 6).

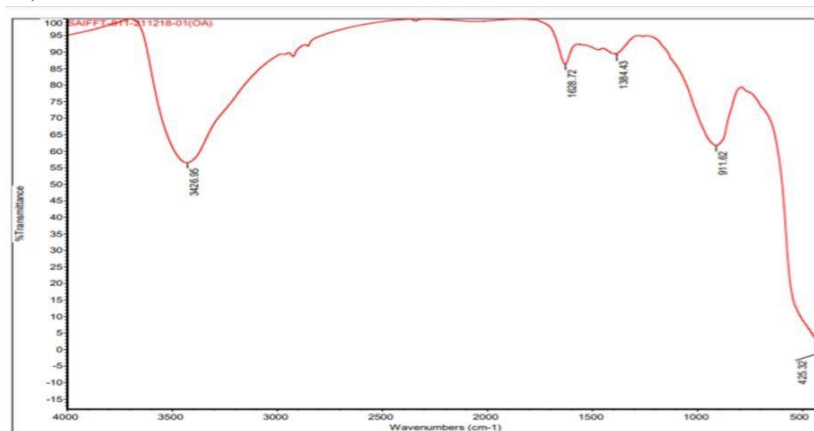


Fig.6: FTIR spectrum of ZnO nanoparticle

3.2.3 SEM

SEM studies was carried out in order to examine the morphology of the prepared ZnO nanoparticles. The SEM images of the obtained ZnO nanoparticles are shown in Figure 7 and it shows somewhat spherical like morphology.[29, 30]

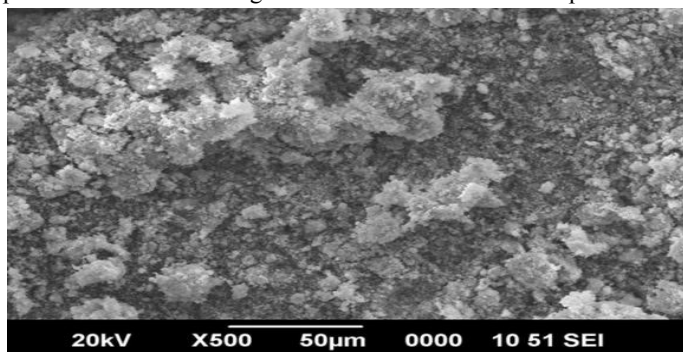


Fig.7 : SEM image of synthesized Zinc Oxide nanoparticles from Zinc Acetate

3.2.4 EDAX

Elemental composition analysis of the samples was conducted through Energy-Dispersive X-ray Spectroscopy (EDAX), a technique employed to ascertain the presence and relative abundance of different elements within the synthesized material. In Figure 8, the EDAX spectrum of the synthesized ZnO nanoparticles is presented, providing a window into the elemental constituents of the sample. Within this spectrum, the characteristic of two essential elements, Zinc and Oxygen, distinctly seen. These peaks signal the elemental composition of the sample, reaffirming the presence of Zinc and Oxygen within the synthesized ZnO nanoparticles. This analysis, therefore, underscores the high purity of the synthesized nanoparticles, as indicated by the presence of only these two elemental components in significant proportions.[31]

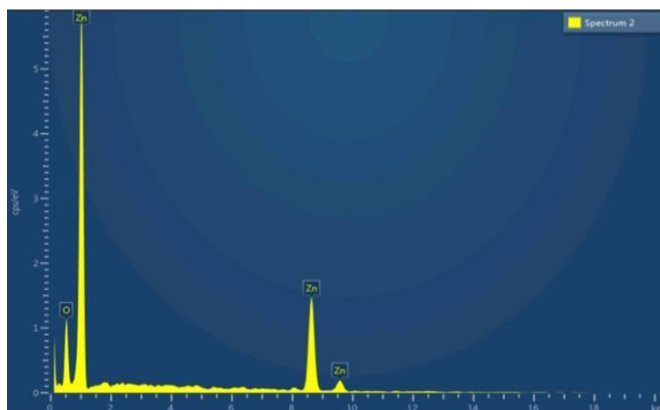


Fig 8: EDAX spectrum of Zinc Oxide nanoparticle

3.3 Characterizations of Copper doped ZnO Nanoparticles

3.3.1 X-ray diffraction

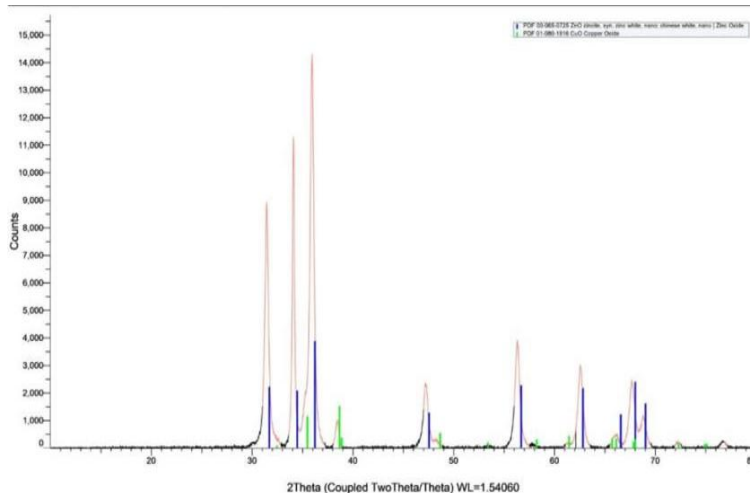


Fig 9: XRD spectrum of synthesized Copper doped Zinc Oxide nanoparticles

Notably in figure 9, a distinctive additional peak emerges at 38.4470 degrees in comparison to the XRD pattern of undoped ZnO. This newly observed peak serves as compelling evidence of copper's successful integration into the ZnO lattice, indicating the presence of a doped material. The average crystal size was determined using Debye Scherrer equation and it was found to be 23.6278 nm.[32, 33]

3.3.2 FTIR Studies

FT-IR Spectroscopy was employed to study the influence of Cu doping on Zn–O bonding (Figure 10). Within this spectrum, a distinctive band emerges, spanning the 400 – 500 cm^{-1} range. This specific band resonates with the pure ZnO reference and is a clear indicator of Zn–O bond formation. Furthermore, the FT-IR spectrum reveals notable absorption peaks at 3379 and 1380 cm^{-1} , which can be ascribed to the O–H stretching of water molecules. The band at 893 cm^{-1} is associated with the alteration in microstructural characteristics, a direct consequence of Copper's introduction into the Zn–O lattice. This observation adds a layer of insight into the subtle yet impactful changes induced by the Copper doping process.[34]

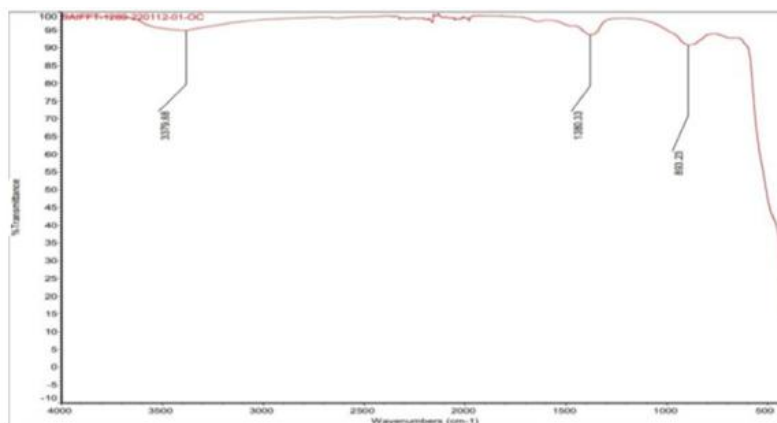


Fig.10: FT-IR spectrum of synthesized Copper doped Zinc Oxide nanoparticles

3.3.3 SEM

The morphological aspects of the Copper-doped ZnO nano powder were extensively examined, as depicted in Figure 11. This visual representation distinctly showcases an intriguing transformation in the morphology, encompassing alterations in particle shape and size, all attributable to the introduction of Cu^{2+} ions into the Zn^{2+} lattice positions. A pronounced distinction is evident in the resultant morphology, characterized by the formation of aggregates. These changes stand in contrast to the undoped ZnO reference. Notably, the incorporation of Cu^{2+} imparts the formation of aggregates highlights the interparticle interactions and spatial arrangement changes induced by the doping process.[35]

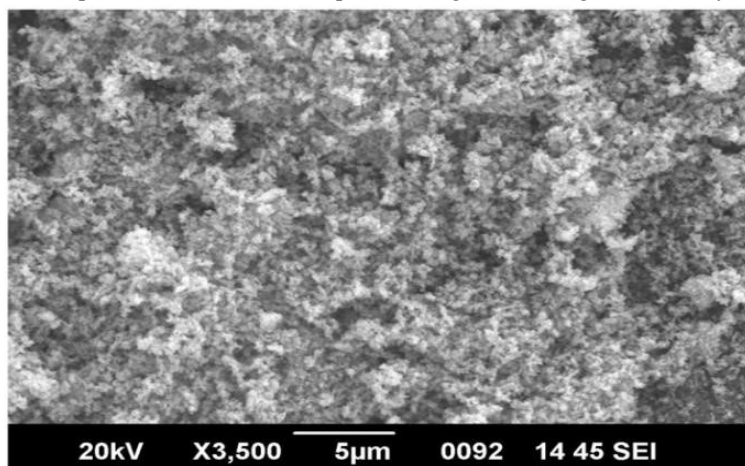


Fig 11: SEM image of synthesized Copper doped Zinc Oxide nanoparticles

3.3.4 EDAX

Illustrated in Figure 12 is the EDAX spectrum showcasing the elemental makeup of the synthesized Copper-doped Zinc Oxide (ZnO) nanoparticles. Prominent within this spectrum are three elements: Zinc, Oxygen, and Copper. This signifies the composition of the synthesized Copper-doped ZnO nanoparticles. The EDAX analysis, therefore, reinforces the high purity of the material, revealing the inclusion of Copper alongside the primary constituents of Zinc and Oxygen that are inherent in undoped ZnO nanoparticles.[36]

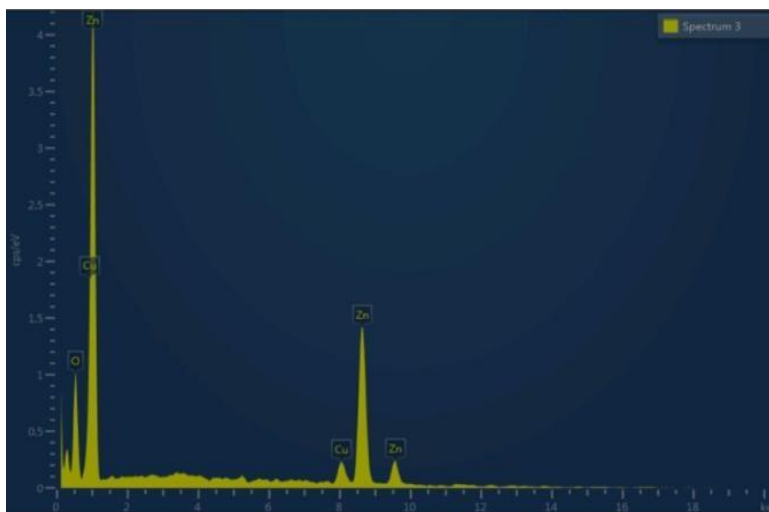


Fig.12: EDAX spectrum of synthesized Copper doped Zinc Oxide nanoparticles

3.4 Antibacterial assay of C-dot@ZnO and C-dot@ZnO-Cu

After incubation of 24 hours, it has been found that C-dot is bacteriosidal against both *E. Coli* and *S.aureus* (Figure 13). C-dot is showing a zone of inhibition of diameter of 1cm against both the bacterial strains. For C-dot@ZnO nanocomposite, the diameter of zone of inhibition for *E.coli* became 1.5 cm whereas for *S.aureus* it became 1.2 cm. Therefore C-dot@ZnO nanocomposite shows more antibacterial activity against *E.coli*. This indicates that the incorporation of ZnO and Cu-doped ZnO has augmented the antibacterial efficiency of the C-dot. When examining the C-dot@ZnO-Cu nanocomposite, an even more pronounced antibacterial effect was evident compared to both C-dot and C-dot@ZnO. The C-dot@ZnO-Cu nanocomposite exhibited enhanced antibacterial activity against *E. coli* with a zone of inhibition of 1.7 cm compared to 1 cm for C-dot, and against *S. aureus* with a zone of inhibition of 1.3 cm compared to 1 cm for C-dot. This nanocomposite exhibited heightened antibacterial activity against both *E. coli* and *S. aureus*. Table 1 shows the antibacterial activity of various samples represented as D, E and F.



(b)

Fig 13 : Images of *S. aureus* and *E. coli* bacteria after incubation

Table 1: Antibacterial activity against *E.coli* and *S.aureus*

SAMPLE	DIAMETER OF ZONE OF INHIBITION	
	<i>E.coli</i>	<i>S.aureus</i>
D) C- DOT	1 cm	1 cm
E) C-dot@ZnO nanocomposite	1.5 cm	1.2 cm
F) C-dot@ZnO-Cu nanocomposite	1.7 cm	cm

IV. CONCLUSION

This research has concentrated on the synthesis, characterization, and application of fluorescent carbon dots derived from prawn shell waste utilizing the hydrothermal method. The thorough characterization of these carbon dots through XRD, TEM, and UV-Visible spectroscopy, along with FTIR analysis confirming the presence of essential functional groups, has revealed their precise size and morphology, signifying their versatile potential for various applications. Additionally, we undertook the synthesis and comprehensive characterization of zinc oxide and copper-doped zinc oxide nanoparticles. The successful incorporation of copper into the zinc oxide lattice was verified through XRD and FTIR analysis, leading to substantial alterations in nanoparticle morphology and elemental composition, as vividly portrayed in SEM and EDAX studies. Of paramount significance is the remarkable discovery of heightened antibacterial activity exhibited by the carbon dot@ZnO-Cu nanocomposite, surpassing the efficacy of carbon dots in isolation and the carbon dot@ZnO composite. This significant enhancement underscores a promising avenue for the development of potent antibacterial agents. This study has ignited a promising trajectory towards the creation of advanced nanocomposite materials endowed with superior antibacterial properties, while simultaneously contributing to sustainable crustacean waste utilization. These developments hold considerable promise for numerous applications and environmental conservation efforts.

V. ACKNOWLEDGMENTS

The authors would like to express their sincere appreciation to SAIF STIC, CUSAT for their invaluable assistance in conducting the chemical analysis.

Funding: The authors are grateful for the financial support in the form of a short-term research grant provided by Prof. N. R. Madhava Menon Interdisciplinary Centre for Research Ethics and Protocols (ICREP), CUSAT, Kerala, India.

REFERENCES

- [1]. Levy, S.B., and Marshall, B.J.N.m.: ‘Antibacterial resistance worldwide: causes, challenges and responses’, 2004, 10, (Suppl 12), pp. S122-S129.
- [2]. Mansuriya, B.D., and Altintas, Z.J.N.: ‘Carbon Dots: Classification, properties, synthesis, characterization, and applications in health care—An updated review (2018–2021)’, 2021, 11, (10), pp. 2525
- [3]. Ghirardello, M., Ramos-Soriano, J., and Galan, M.C.J.N.: ‘Carbon dots as an emergent class of antimicrobial agents’, 2021, 11, (8), pp. 1877
- [4]. Das, R., Bandyopadhyay, R., and Pramanik, P.J.M.t.c.: ‘Carbon quantum dots from natural resource: A review’, 2018, 8, pp. 96-109
- [5]. Feng, X., Jiang, Y., Zhao, J., Miao, M., Cao, S., Fang, J., and Shi, L.J.R.A.: ‘Easy synthesis of photoluminescent N-doped carbon dots from winter melon for bio-imaging’, 2015, 5, (40), pp. 31250-31254
- [6]. Hu, Y., Zhang, L., Li, X., Liu, R., Lin, L., Zhao, S.J.A.S.C., and Engineering: ‘Green preparation of S and N Co-doped carbon dots from water chestnut and onion as well as their use as an off-on fluorescent probe for the quantification and imaging of coenzyme A’, 2017, 5, (6), pp. 4992-5000
- [7]. Humaera, N.A., Fahri, A.N., Armynah, B., and Tahir, D.J.L.: ‘Natural source of carbon dots from part of a plant and its applications: A review’, 2021, 36, (6), pp. 1354-1364
- [8]. Jelinek, R.J.C.q.d.S.I.P., Cham: ‘Carbon quantum dots’, 2017, pp. 29-46

- [9]. Liu, J., Li, R., and Yang, B.J.A.C.S.: 'Carbon dots: A new type of carbon-based nanomaterial with wide applications', 2020, 6, (12), pp. 2179-2195
- [10]. Yang, J., Zhang, X., Ma, Y.-H., Gao, G., Chen, X., Jia, H.-R., Li, Y.-H., Chen, Z., Wu, F.-G.J.A.a.m., and interfaces: 'Carbon dot-based platform for simultaneous bacterial distinguishment and antibacterial applications', 2016, 8, (47), pp. 32170-32181
- [11]. Muthu, M., Gopal, J., Chun, S., Devadoss, A.J.P., Hasan, N., and Sivanesan, I.J.A.: 'Crustacean waste-derived chitosan: Antioxidant properties and future perspective', 2021, 10, (2), pp. 228
- [12]. Xu, Y., Gallert, C., Winter, J.J.A.M., and Biotechnology: 'Chitin purification from shrimp wastes by microbial deproteination and decalcification', 2008, 79, pp. 687-697
- [13]. Gedda, G., Lee, C.-Y., Lin, Y.-C., Wu, H.-f.J.S., and Chemical, A.B.: 'Green synthesis of carbon dots from prawn shells for highly selective and sensitive detection of copper ions', 2016, 224, pp. 396-403
- [14]. Raja, A., Ashokkumar, S., Marthandam, R.P., Jayachandiran, J., Khatiwada, C.P., Kaviyarasu, K., Raman, R.G., Swaminathan, M.J.J.o.P., and Biology, P.B.: 'Eco-friendly preparation of zinc oxide nanoparticles using *Tabernaemontana divaricata* and its photocatalytic and antimicrobial activity', 2018, 181, pp. 53-58
- [15]. Joshi, P., Chakraborti, S., Chakrabarti, P., Singh, S.P., Ansari, Z., Husain, M., and Shanker, V.J.S.o.A.M.: 'ZnO nanoparticles as an antibacterial agent against *E. coli*', 2012, 4, (1), pp. 173-178
- [16]. Liang, J., Li, W., Chen, J., Huang, X., Liu, Y., Zhang, X., Shu, W., Lei, B., and Zhang, H.J.A.A.B.M.: 'Antibacterial activity and synergetic mechanism of carbon dots against gram-positive and-negative bacteria', 2021, 4, (9), pp. 6937-6945
- [17]. Li, P., Sun, L., Xue, S., Qu, D., An, L., Wang, X., and Sun, Z.J.S.: 'Recent advances of carbon dots as new antimicrobial agents', 2022, 3, (2), pp. 226-248
- [18]. Mounika, T., Belagali, S.L., and Vadiraj, K.J.E.M.R.: 'Synthesis and characterization of zinc oxide quantum dots using an acidic precursor', 2020, 9, (2), pp. 378-382
- [19]. Thiawong, T., Onlaor, K., Chaithanatkun, N., and Tunhoo, B.: 'Preparation of copper doped zinc oxide nanoparticles by precipitation process for humidity sensing device', in Editor (Ed.)^(Eds.): 'Book Preparation of copper doped zinc oxide nanoparticles by precipitation process for humidity sensing device' (AIP Publishing, 2018, edn.), pp.
- [20]. Gao, D., Zhao, P., Lyu, B., Li, Y., Hou, Y., and Ma, J.J.A.O.C.: 'Carbon quantum dots decorated on ZnO nanoparticles: An efficient visible-light responsive antibacterial agents', 2020, 34, (8), pp. e5665
- [21]. Emam, A., Loutfy, S.A., Mostafa, A.A., Awad, H., and Mohamed, M.B.J.R.a.: 'Cyto-toxicity, biocompatibility and cellular response of carbon dots-plasmonic based nano-hybrids for bioimaging', 2017, 7, (38), pp. 23502-23514
- [22]. Surendran, P., Lakshmanan, A., Vinitha, G., Ramalingam, G., and Rameshkumar, P.J.L.: 'Facile preparation of high fluorescent carbon quantum dots from orange waste peels for nonlinear optical applications', 2020, 35, (2), pp. 196-202
- [23]. Nguyen, H.A., Srivastava, I., Pan, D., and Gruebele, M.J.A.N.: 'Unraveling the fluorescence mechanism of carbon dots with sub-single-particle resolution', 2020, 14, (5), pp. 6127-6137
- [24]. Sailaja Prasannakumaran Nair, S., Kottam, N., and SG, P.K.J.J.o.F.: 'Green synthesized luminescent carbon nanodots for the sensing application of Fe³⁺ ions', 2020, 30, pp. 357-363
- [25]. Dager, A., Uchida, T., Maekawa, T., and Tachibana, M.J.S.r.: 'Synthesis and characterization of mono-disperse carbon quantum dots from fennel seeds: photoluminescence analysis using machine learning', 2019, 9, (1), pp. 14004
- [26]. Linehan, K., and Doyle, H.J.R.A.: 'Solution reduction synthesis of amine terminated carbon quantum dots', 2014, 4, (24), pp. 12094-12097
- [27]. Kalpana, V., Kataru, B.A.S., Sravani, N., Vigneshwari, T., Panneerselvam, A., and Rajeswari, V.D.J.O.: 'Biosynthesis of zinc oxide nanoparticles using culture filtrates of *Aspergillus niger*: Antimicrobial textiles and dye degradation studies', 2018, 3, pp. 48-55

- [28]. Arefi, M.R., and Rezaei-Zarchi, S.J.I.j.o.m.s.: ‘Synthesis of zinc oxide nanoparticles and their effect on the compressive strength and setting time of self-compacted concrete paste as cementitious composites’, 2012, 13, (4), pp. 4340-4350
- [29]. Shah, S.N., Ali, S.I., Ali, S.R., Naeem, M., Bibi, Y., Ali, S.R., Raza, S.M., Khan, Y., Sherwani, S.K.J.J.o.B., and Sciences, A.: ‘Synthesis and characterization of zinc oxide nanoparticles for antibacterial applications’, 2016, 12
- [30]. Naseer, M., Aslam, U., Khalid, B., and Chen, B.J.S.R.: ‘Green route to synthesize Zinc Oxide Nanoparticles using leaf extracts of Cassia fistula and Melia azadarach and their antibacterial potential’, 2020, 10, (1), pp. 9055
- [31]. Singh, D., Pandey, D., Yadav, R., and Singh, D.J.P.: ‘A study of nanosized zinc oxide and its nanofluid’, 2012, 78, pp. 759-766
- [32]. Mukhtar, M., Munisa, L., and Saleh, R.: ‘Co-precipitation synthesis and characterization of nanocrystalline zinc oxide particles doped with Cu 2+ ions’, 2012
- [33]. Kale, G., Arbuj, S., Kawade, U., Kadam, S., Nikam, L., and Kale, B.J.J.o.M.S.M.i.E.: ‘Paper templated synthesis of nanostructured Cu–ZnO and its enhanced photocatalytic activity under sunlight’, 2019, 30, pp. 7031-7042
- [34]. Sable, P.B., Thabet, N., Yaseen, J., Botewad, S.N., Gaikwad, D., Joshi, A., and Dharne, G.: ‘Effects on structural, functional groups and photo luminance properties of copper doped zinc oxide nanoparticles’, in Editor (Ed.)^(Eds.): ‘Book Effects on structural, functional groups and photo luminance properties of copper doped zinc oxide nanoparticles’ (IOP Publishing, 2020, edn.), pp. 012016
- [35]. Rahmati, A., Balouch Sirgani, A., Molaei, M., and Karimipour, M.J.T.E.P.J.P.: ‘Cu-doped ZnO nanoparticles synthesized by simple co-precipitation route’, 2014, 129, pp. 1-7
- [36]. Debanath, M., Borah, S., and Karmakar, S.: ‘Study of Structural and Optical Properties of Undoped and Cu Doped ZnO Nanostructures (NSs) in PVP Matrix by Wet Chemical Route’, 2015, 2(20):1740-1744.